DOI: 10.1002/chem.200600551

Theoretical Investigation of the Second-Order Nonlinear Optical Properties of Helical Pyridine–Pyrimidine Oligomers

Edith Botek,[a] Frédéric Castet,[b] and Benoît Champagne*[a]

Abstract: The structure and second-order nonlinear optical properties of a series of helical pyridine–pyrimidine oligomers recently synthesized by Barboiu and Lehn have been investigated theoretically by combining molecular mechanics and quantum chemistry approaches. In the absence of substituents, the hyper-Rayleigh scattering response (β_{HRS}) and the projection of the first hyperpolarizability on the dipole moment ($\beta_{\parallel}$) exhibit periodic variations with chain length, but these nonlinear optical responses remain small. The first hyperpolarizabilities can, however, be enhanced by adding substituents. The greatest enhancement is obtained by substituting the pyrimidine groups by donor groups. Moreover, regular distributions of the donor groups around the helices enable the design of supramolecular structures exhibiting dipolar, octupolar or Λ-shaped nonlinear optical characters, evident from the values of the depolarization ratios in hyper-Rayleigh scattering. Therefore this theoretical investigation demonstrates the potential of helical structures for the organization of chromophores in such a way that they exhibit large and specific second-order nonlinear optical responses.

Keywords: helical structures · nitrogen heterocycles · nonlinear optics · substituent effects

Introduction

The design of molecular and supramolecular systems for application in nonlinear optical (NLO) devices has been enriched over the last decades by the synthesis and characterization of helical (chiral) structures.[1] Helices are in fact present in many fields of research ranging from the genetic encoding in biomacromolecules[2] to the enhancement of electrical conductivity in materials science.[3] Various possibilities exist for obtaining molecules with a helical conformation,[4] from the synthesis of rigid molecules in which the minimization of steric strains leads to helix formation, to flexible molecules adopting a helical conformation as a result of stabilizing intramolecular noncovalent interactions, to the formation of supramolecular aggregates with a helical superstructure.[5] Moreover, helical–linear strand transitions, associated with local conformational modifications induced by internal (chain length) or external stimuli (recognition of ions, pH), have been studied to gain a better understanding of biopolymers[6,7] as well as in view of designing supramolecular catalysts.[8] In many cases, structures found in nature constitute the source of inspiration for the elaboration of new artificial architectures with targeted properties. The design of nonbiological structures often relies on the molecular self-organization of superstructures[9] and focuses principally on applications in nanotechnology, optics, and electronics.[10–12] Among these systems, conjugated helical molecules composed of *ortho*-fused aromatic rings, called (homo- or hetero-) helicenes, have been extensively studied, both experimentally[13–18] and theoretically.[19–21] In particular, strategies have been proposed to enhance their second-order NLO responses. Chiral induction and amplification mechanisms have also been studied in a variety of (helical) polymers bearing chiral groups[22] as well as in chiral columnar stacks of C_3-symmetry molecules.[23]

Starting from the principle that 2,2′-bipyridine adopts an s-*trans* conformation, Lehn and co-workers proposed several helical structures based on heterocycles,[24–29] including pyridine–pyridazine, pyridine–naphtyridine, and pyridine–pyrimidine units, which can be considered as coiled molecular wires of nanometric size, possessing electron-acceptor properties associated with the nature of their subunits and sub-

[a] Dr. E. Botek, Dr. B. Champagne
Laboratoire de Chimie Théorique Appliquée
Facultés Universitaires Notre-Dame de la Paix
Rue de Bruxelles, 61, 5000 Namur (Belgium)
Fax.: (+32) 81-724-567
E-mail: benoit.champagne@fundp.ac.be

[b] Dr. F. Castet
Laboratoire de Physico-Chimie Moléculaire
UMR 5803 CNRS—Université de Bordeaux I
Cours de la Libération, 351, 33405 Talence CEDEX (France)

stituents. For some of these species, the helical structure changes to accommodate the complexation of ions into coils or double helices. Moreover, their self-organization into helices provides a way of positioning peripheral substituents in well-defined spatial arrangements relative to one another,[24] a condition for achieving substantial macroscopic second-order NLO responses. Indeed, without a structuring strength, the efficient push–pull π-conjugated systems tend to pack in a centrosymmetric way, giving rise to vanishing macroscopic second-order NLO responses. Like hydrogen bonding,[30] the formation of supramolecular structures appears to be a promising way of maximizing the second-order NLO responses. This is the aspect we address in the present paper by carrying out a theoretical investigation of the NLO properties of pyridine–pyrimidine oligomers (Scheme 1). In particular, their second-order NLO responses are evaluated and analyzed as a function of the size of the helix as well as of the nature, concentration, and relative positions of the substituents. First we investigate the intrinsic NLO properties of pyridine–pyrimidine helices. Then we address the effects of substitutions by donor and acceptor groups. The next section describes the main theoretical and computational aspects, with the results and discussions given in the later sections.

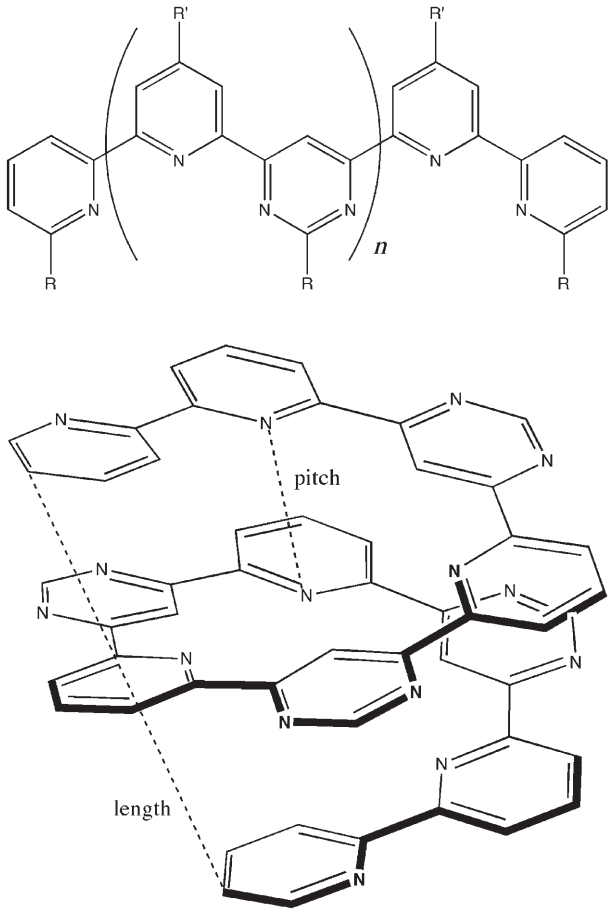

Scheme 1. Extended, linear structure (top) and helical winding (bottom, R = R′ = H and $n = 4$) of the pyridine–pyrimidine strands. The distance between the extremities, referred to as the *length* and the distance between two successive turns, abusively called the *pitch*, are also defined.

Computational Methods

Geometry optimizations were performed either using molecular mechanics (MM) within standard force fields (MM2*,[31] MM3*,[32] AMBER*[33] and OPLS-AA[34] available in the MacroModel suite[35]) or quantum mechanics within the semiempirical AM1,[36] PM3,[37] and PM5[38] Hamiltonians.

The first hyperpolarizability (β) tensor—defined by using the Taylor series expansion of the field-dependent dipole moment—was evaluated at the time-dependent Hartree-Fock (TDHF) level[39] by using the AM1 Hamiltonian. This approximation was demonstrated in a series of works[40–42] to be a good choice combining both the quality of the results and the sparing of computational resources for the investigation of NLO responses in medium- and large-size systems. Two second-order NLO responses, derived from specific sums of the first hyperpolarizability tensor components, were investigated in the present work. The first one corresponds to the projection of the vector part of β on the dipole moment vector, as shown in Equation (1), in which $||\mu||$ is the norm of the dipole moment and μ_i and β_i are the components of the μ and β vectors.

$$\beta_{\parallel}(-2\omega;\omega,\omega) = \beta_{\parallel} = \frac{3}{5}\sum_i \frac{\mu_i}{||\mu||}\sum_j (\beta_{ijj}+\beta_{iji}+\beta_{jii}) = \frac{3}{5}\sum_i \frac{\mu_i\beta_i}{||\mu||} \quad (1)$$

The second property is related to the hyper-Rayleigh scattering intensity for plane-polarized incident light and observation made perpendicular to the propagation plane, [Eq. (2)], with the associated depolarization ratio (DR) given by Equation (3). Full expressions for $\langle\beta^2_{ZZZ}\rangle$ and $\langle\beta^2_{XZZ}\rangle$ without assuming Kleinman's conditions can be found in reference [43]; these correspond to an orientational average of the β tensor components, which contrary to the sums of Equation (1) contains β_{ijk} components in which i, j, and k are all different.

$$\beta_{\mathrm{HRS}}(-2\omega;\omega,\omega) = \sqrt{\{\langle\beta^2_{ZZZ}\rangle + \langle\beta^2_{XZZ}\rangle\}} \quad (2)$$

$$\mathrm{DR} = \frac{\langle\beta^2_{ZZZ}\rangle}{\langle\beta^2_{XZZ}\rangle} \quad (3)$$

The MacroModel program[44] was employed for the structure optimizations while the hyperpolarizabilities were calculated using the MOPAC 2000[45] program. A typical wavelength of 1064 nm was adopted in all β calculations.

Results and Discussion

Geometrical structures of the pyridine–pyrimidine helices: The first objective of this work is the validation of a method for optimizing the geometry of the pyridine–pyrimidine strands. This is accomplished by comparing optimized structures obtained at different levels of approximation with the crystal structure of the compound with $n = 8$ and R = H taken from reference [24]. Its unit cell contains two molecules but only one enantiomeric form, in which the helix makes three turns. The torsion angle between consecutive pyridine–pyrimidine rings lies within $11 \pm 3°$, the helical

pitch is 3.63 Å, and the interior void has a diameter of 2 Å. The last parameter is obtained by projecting the atoms onto a basal plane, while taking into account the van der Waals radii of diagonally located N and C–H sites. This structure is represented in Figure 1.

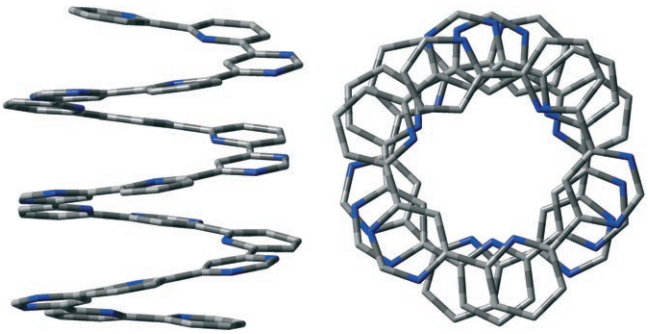

Figure 1. Side and top views of the helical pyridine–pyrimidine oligomer ($n=8$) taken from reference [24].

Table 1 reports the most representative geometrical features of the $n=8$ (R = H) compound as optimized with the different theoretical approaches in comparison with experimental data. All structures optimized within MM are very similar to the crystal structure (Figure 1), with the total superposition rate—estimated by evaluating the root-mean-square difference between the Cartesian coordinates—ranging from 0.002 Å (OPLS-AA) to 0.378 Å (MM2*). The structure optimized at the MM/OPLS-AA level is displayed in Figure 2A. Three pyridine–pyrimidine units make slightly more than one helical turn so that the structure does not exactly exhibit C_3 symmetry. A similar situation was found for the helicenes and heliphenes, with a noticeable difference for the (approximate) number of units per helical turn: three for the pyridine–pyrimidine oligomers, but six for the helicenes and heliphenes[19] although the number of aromatic rings is similar. Further information about the relationship between the chemical motif and the number of units per helical turn can be found in the works by Huc and collaborators.[6]

Table 1. Comparison between calculated and experimental structural parameters of the pyridine–pyrimidine oligomers containing eight units for different levels of approximation.

Method of calculation	Pitch [Å]	Mean torsion angle [°]	length [Å]
MM/MM2*	3.74	9.31	12.09
MM/MM3*	3.74	8.53	13.05
MM/AMBER*	3.55	8.27	12.75
MM/OPLS-AA	3.76	8.90	12.59
PM3	5.30	11.70	14.66
AM1	5.64	12.86	15.31
PM5	5.59	12.19	14.86
AM1 (bis)	11.15	42.00	42.02
experiment (crystal)	3.63	8.64	12.65

When semiempirical schemes are used for geometry optimization, several differences occur including 1) larger helical pitches and, therefore, more extended chains; 2) an increase in the torsion angles by about a factor of 3; and 3) the lack of regularity of the helical shape, which translates into the alternation of inter-ring torsion angles: one negative ($-32.5\pm2°$) followed by two positive ($33.8\pm9°$) angles. This is illustrated in Figure 2B for the case of an optimization adopting the PM3 Hamiltonian. Although there are no significant differences between the semiempirical Hamiltonians, the structural parameters obtained with the most recent PM5 parameterization are intermediate between the PM3 and AM1 approaches. DFT calculations perform only slightly better than the semiempirical schemes, providing poorer structural parameters than the MM schemes.[46]

Interestingly, by using semiempirical Hamiltonians, another stable structure was also determined. As shown in Figure 2C for an AM1 Hamiltonian, this structure, referred to as the bis-structure, is much more extended and only 2.5 pyridine–pyrimidine units are necessary to make a full helical turn. At the AM1 level, this bis-structure is only 1.3 kJ mol^{-1} higher in energy than the more compact one, whereas when the PM3 and PM5 Hamiltonians are used, this difference increases to 5.4 kJ mol^{-1}. In view of all these findings the MM/OPLS-AA level appears to be the most suitable method for the geometry optimization of pyridine–pyrimidine oligomers, and subsequently this method was adopted for the whole investigation. Nevertheless, using other MM schemes for geometry optimizations would affect slightly the β_{HRS} values, but not the qualitative trends as exemplified by the 12–17% variation of β_{HRS} when going from the OPLS-AA to the MM3* or AMBER* structures.

Nonlinear optical properties of pyridine–pyrimidine oligomers: The second-order NLO responses have been calculated for increasingly large (non-substituted, R, R′ = H) pyridine–pyrimidine oligomers. Figure 3 sketches the evolution of the coherent ($\beta_{\parallel}$) and incoherent (β_{HRS}) second-order NLO responses in comparison with the norm of the dipole moment ($||\mu||$) for n ranging from 3 to 28. The evolution of $||\mu||$ and $\beta_{\parallel}$ exhibit some regularity, which is better evidenced by distinguishing three sets of chains as a function of the number of units: $3m$, $3m+1$, and $3m+2$ units (Figure 4). This quasi-order-3 periodicity finds its origin in the geometrical structure, displaying an axis almost of order 3. In addition to these rapid variations of $||\mu||$ and $\beta_{\parallel}$ with n, Figure 4 enables the observation that the smooth variations of properties for the three subsets of systems also exhibit a periodic-like behavior, albeit of large period.

These two periodicities, and in particular the variation having the largest period, are further exemplified by considering the *radial* angle formed by the helix extremities. To determine this angle, the geometrical structure is first projected on the plane perpendicular to the helical axis and then the radial displacement of one extremity ring with respect to the other is measured. Figure 5 demonstrates that the three series of points can be placed side by side to re-

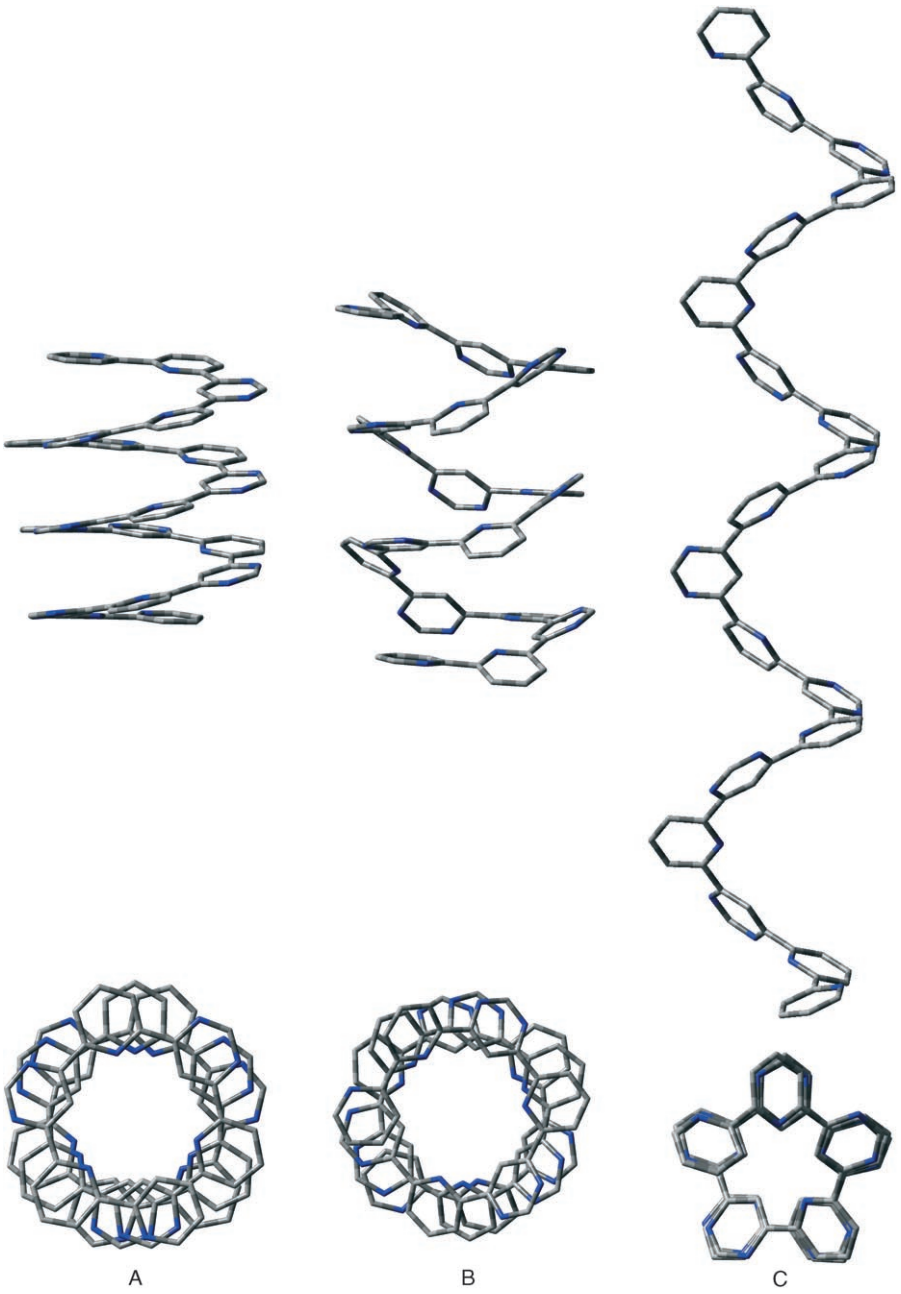

Figure 2. Side (top) and top (bottom) views of structures optimized at different levels of approximation. A) MM/OPLS-AA, B) PM3, and C) AM1 (bis-structure).

construct a unique variation of the radial displacement from 0 to 2π, defining therefore a period of about 75/3 units. Thus, the radial displacement of a $3m$ helix containing x+25 (x+50) units (with x an integer) is similar to the radial displacement of a $3m$+1 ($3m$+2) helix with x units. Hence, the same correspondence between the $3m$, $3m$+1, and $3m$+2 helices occurs for the NLO properties.

So, in the (small) chains containing $3m-1$ units the helices are made of full turns, which can be associated with a reduced radial asymmetry and therefore to a small dipole moment. Of course, this has to be taken with some scepticism, first because three units make slightly more than one helical turn and second because of the presence of the chain extremities: at one extremity there is an additional pyridine ring, whereas at the other, the pyridine–pyrimidine unit is replaced by a bipyridine moiety. Then the evolution of $\beta_{\parallel}$ is not exactly in phase with the variation in the dipole moment. Indeed, up to $n=9$, the smallest $\beta_{\parallel}$ values correspond to chains containing $3m$ units, while beyond $n=9$ the smallest $\beta_{\parallel}$ values are obtained for the $3m$+2 subset. This is associated with the change of sign of the $3m$+2 $\beta_{\parallel}$ values between $n=8$ and $n=11$. In turn, this change of sign finds its origin in the evolution of the dipole moment with the helix size (Figure 4), which decreases for $n<10$ and increases otherwise, going from a situation in which the μ and β vectors are parallel to a situation in which they are antiparallel. Moreover, for extended systems ($n>9$), the largest dipole moment amplitudes are generally displayed by the chains with $3m$ units, whereas the chains with $3m$+1 units present, in most cases, the largest $\beta_{\parallel}$. Based on Figures 4 and 5, one can expect similar behaviors in longer helices, besides the fact that, with a period of about 25, the three subsets of chains interchange. The relation between $||\mu||$ and $\beta_{\parallel}$ is therefore more complex than in helicenes and heliphenes, in which they evolve in-phase and out-of-phase, respectively.[20] Moreover, as for the latter systems, the first hyperpolarizability of pyridine–pyrimidine oligomers is mostly radial.

The behavior of β_{HRS} with chain length is different; the variations also follow a regular pattern, characterized by a unique periodicity of about 25 units, substantiating the fact that the main impact of the periodicity of order three concerns the relative orientation of the vectorial quantities, and therefore $\beta_{\parallel}$. β_{HRS} attains a maximum for $n=8$ and a minimum for $n=21$. Thus, the system characterized in reference [24] presents the optimal size for maximizing β_{HRS}. For

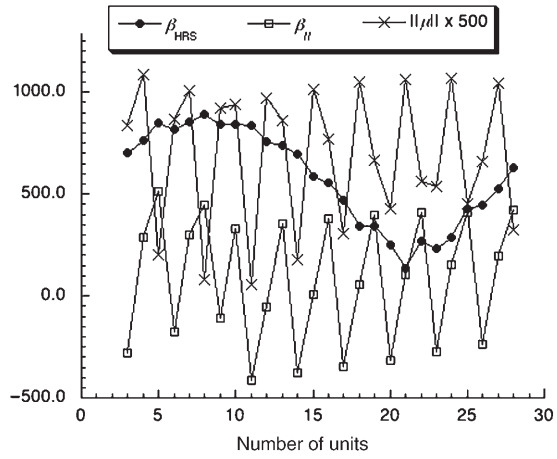

Figure 3. Evolution of β_{HRS}, $\beta_{\parallel}$ (in au, 1.0 au of $\beta = 3.6213 \times 10^{-42}\ m^4 V^{-1} = 3.206361 \times 10^{-53}\ C^3 m^3 J^{-2} = 8.6392 \times 10^{-33}$ esu), and $||\mu||$ (in D × 500) as a function of the number of pyridine–pyrimidine units.

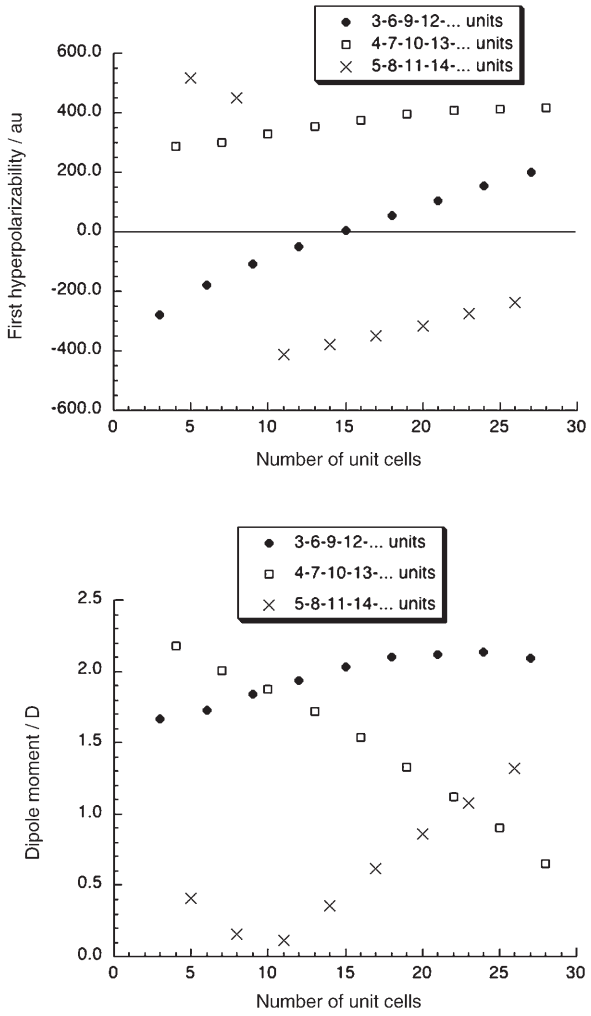

Figure 4. Evidence of the three-unit periodicity of the evolution of $\beta_{\parallel}$ (top, in au) and $||\mu||$ (bottom, in D) with the helix size.

chains containing fewer than 19 units, the DR is almost constant and is close to 1.5, the value characterizing octupolar systems (Figure 6). For $n = 22$, DR is equal to 5.75, which is

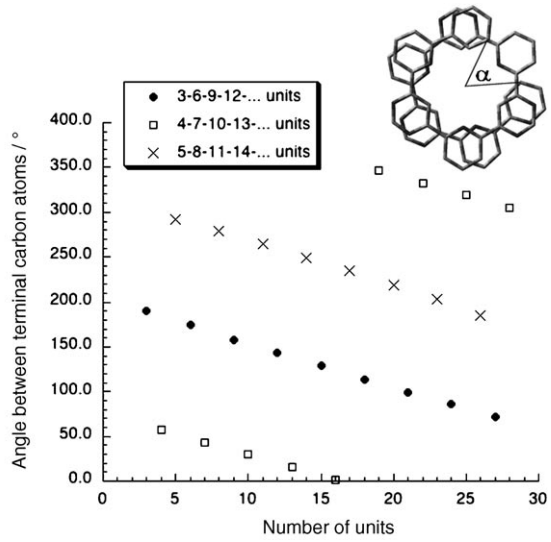

Figure 5. Evolution with the length of the chain of the radial displacement (α, in degrees) between the terminal rings of the helix.

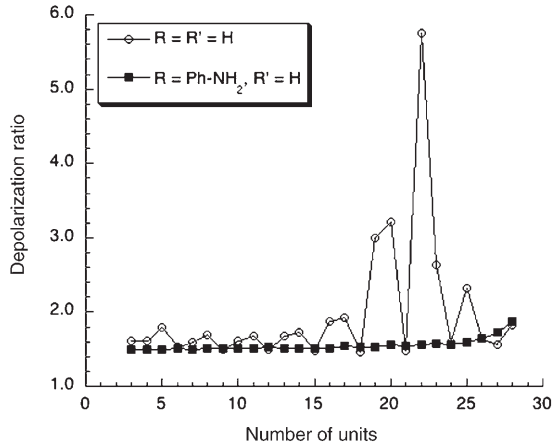

Figure 6. Depolarization ratio as a function of the number of pyridine–pyrimidine units with and without aniline substituents on the pyrimidine rings.

typical of dipolar chromophores. This size corresponds to the seven-turn helix presenting the smallest β_{HRS} and β tensor components, although also the largest $||\mu||$ values, so that a (residual) dipolar NLO character seems to be associated with a structural octupolar character.

Substitution effects on the structural and NLO properties of pyridine–pyrimidine oligomers: Since the first hyperpolarizability values of the helices with R = R′ = H remain small and do not show an ad hoc size dependence in order to lead to substantially larger NLO responses in longer chains, in a second step the effects of substituting the pyridine–pyrimidine helices on β_{HRS} have been investigated. As justified later, donor or acceptor groups (R) were placed on the pyrimidine rings, leaving the pyridine rings nonsubstituted. In addition to cases in which all the pyrimidine rings are substi-

tuted, partial although regular substitution patterns have also been considered (Figure 7). Full substitution (3/3) gives rise to an octupolar-like structure, such as in crystal violet.[47]

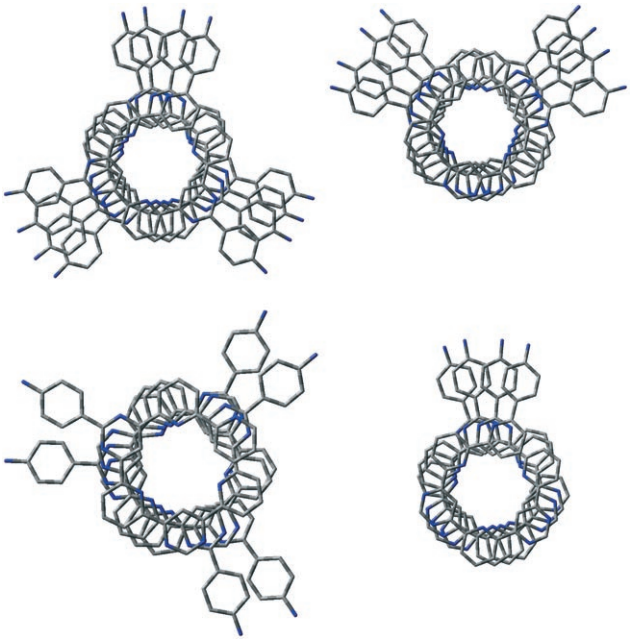

Figure 7. Top views of structures optimized at the MM/OPLS-AA level as a function of the degree of substitution: 3/3 (top left), 2/3 (top right), 1/2 (bottom left), and 1/3 (bottom right). The 3/3 substitution rate corresponds to the full substitution of the R sites (see Scheme 1).

Table 2. Structural parameters optimized at the MM/OPLS-AA level for oligomers containing ten units and different substituents on the pyrimidine rings. For the definition of the pitch and the length, see Scheme 1.

R	Pitch [Å]	Mean torsion angle [°]	Length [Å]
H	3.76	9.0	14.18
CHO	3.84	9.8	13.85
NO_2	3.81	9.9	13.79
OMe	3.83	8.7	14.45
NH_2	3.74	8.4	14.49
Ph–NO_2	3.73	8.2	15.20
Ph–NH_2	3.77	8.8	14.40
Ph–NH_2 (2/3)	3.74	9.0	14.32
Ph–NH_2 (1/2)	3.74	9.2	14.09
Ph–NH_2 (1/3)	3.75	9.1	14.16

Table 3. Substituent effects on β_{HRS} (au) for pyridine and pyrimidine as well as for the pyridine–pyrimidine oligomers containing ten units and substituents on the pyrimidine ring. The resulting intramolecular charge transfers (CT) between the substituents and the rings are also given [$Q = Q$(R) in au]. The quantities in parentheses determine the impact of the helical structure on the β per pyrimidine ring and are given by $\beta(n{=}10)/[12{\times}\beta$(pyrimidine–R)].

R	H	CHO	NO_2	OMe	NH_2
β_{HRS} (pyridine-R)	22	85	29	122	288
CT Q(pyridine-R)	0.14	0.04	-0.13	-0.02	0.05
β_{HRS} (pyrimidine-R)	15	28	167	192	360
CT Q(pyrimidine-R)	0.19	0.13	-0.03	0.04	0.12
β_{HRS} ($n=10$, pyrimidine-R)	846 (4.70)	608 (1.81)	1021 (0.51)	990 (0.43)	1653 (0.38)

This octupolar-like structure remains when every other substituent is removed (substitution rate of 1/2). To get all substituents on the same side of the helix, every third site has to be substituted (substitution rate of 1/3). In this structure the donor/acceptor axes of the substituents are almost aligned so that the dipolar character of the structure is maximized. Finally, the 2/3 substitution rate leads to a supramolecular Λ-shape lateral packing of the chromophores.[48–49]

Geometry optimizations carried out at the MM/OPLS-AA level of approximation show that the variation of the radial displacements in the $3m$, $3m+1$, and $3m+2$ series are smaller than in the case of the nonsubstituted helices. Indeed, by going from 3 to 27 units, the radial displacement goes from 185° to 109°, with a periodicity of about 38 units. The main geometrical parameters of these structures are listed in Table 2. Substitutions by mesomeric donor groups (OMe and NH_2) lead to a decrease of the torsion angle by 0.2–0.5°, whereas the opposite is found for acceptor groups (CHO and NO_2). Other geometrical variations are small and less systematic.

To determine the preferential sites for substitution with donor or acceptor groups, preliminary investigations were carried out on the substitution effects for the pyridine and pyrimidine molecules (Table 3). For both rings, adding a donor (NH_2, OMe) provides larger β_{HRS} values than adding an acceptor, as expected from the electro-attracting character of the rings. Indeed, for comparison, in the case of monosubstituted benzenes, the ordering of the β magnitude is $NO_2 > NH_2 > CHO > OMe$.[50] Following previous investigations,[40] the β magnitudes were compared to the amplitudes of the intramolecular charge transfer (CT) evaluated using the AM1 Hamiltonian within the Coulson population analysis. However, no clear relationship with the amplitude of the intramolecular CT, evaluated as the sum of the atomic charges of the substituents, was observed for the electronic ground state. This is probably a consequence of the competition between inductive and mesomeric effects, both important for the intramolecular CT amplitude, whereas β is mostly dominated by mesomeric effects. Moreover, for strong donors and acceptors, it is advantageous to substitute the pyrimidine rather than the pyridine ring. The amplitude of the β_{HRS}(pyrimidine–R)/β_{HRS}(pyridine–R) ratio ranges from 0.33 (CHO) to 5.76 (NO_2). This stronger attracting character of the pyrimidine ring can be related to the position of substitution. Indeed, the substituted site is close to the nitrogen atoms of the pyrimidine, whereas it is on the opposite side of the ring in the case of pyridine substitution (Scheme 1).

The first hyperpolarizabilities were calculated for the $n=10$ oligomer bearing substituents on the pyrimidine rings (Table 3). The results are rationalized as a function of the

ratio between the β_{HRS} value of the helix and 12 times (corresponding to the number of R substituents) the β_{HRS} value of the substituted pyrimidine molecule. This ratio ranges from 0.38 ($R=NH_2$) to 4.70 ($R=H$), showing the largest damping of β_{HRS} for cases in which the substituted pyrimidine unit presents the largest β_{HRS} value. This can be related to the effect on β when packing D/A (donor/acceptor) chromophores. Indeed, when packing D/A compounds laterally, both dressing and local field effects are detrimental to the first hyperpolarizability.[41] As a consequence of these packing effects, the ordering of the β_{HRS} magnitude is modified when going from the molecular units to the oligomers containing ten units. However, the largest hyper-Rayleigh response is still associated with substitutions by amino groups.

In subsequent work bigger substituents were used, such as Ph–NH_2 and Ph–NO_2, prototypical representatives of electron-donating and electron-withdrawing groups (Table 4).

Table 4. Effects on β_{HRS} (au) induced by substituting the pyridine and pyrimidine rings by the *p*-anilino or *p*-nitrophenyl groups as a function of the position and rate of substitution. For the molecular units, the corresponding charge transfer between the substituents and the rings are also given while the depolarization ratios are provided for the helical oligomers. The quantities in parentheses determine the impact of the helical structure on the β per pyrimidine ring and is given by $\beta(n=10)/[12\times\beta(\text{pyrimidine-R})]$.

	Ph–NO_2 3/3[a]	Ph–NH_2 3/3[a]	Ph–NH_2 2/3[a]	Ph–NH_2 1/3[a]	Ph–NH_2 1/2[a]
β_{HRS} (pyridine-R)	372	1335			
CT Q(pyridine-R)	-0.01	0.02			
β_{HRS} (pyrimidine-R)	105	2218			
CT Q(pyrimidine-R)	0.06	0.10			
β_{HRS} ($n=10$,	487	5956	6081	5003	4801
pyrimidine-R)	(0.39)	(0.22)	(0.34)	(0.56)	(0.36)
DR	1.68	1.52	3.34	4.89	1.61

[a] Substitution rate.

The difference between donor and acceptor substitutions is larger relative to the results given in Table 3. However, there is again a preference to substitute the pyrimidine ring rather than the pyridine ring, and to substitute by an electron-donating group rather than by an electron-withdrawing moiety. The first hyperpolarizability was then evaluated for the fully substituted oligomer with ten units as well as for structures with partial (1/3, 1/2, and 2/3) substitution patterns. When replacing NH_2 by Ph–NH_2 substituents, β_{HRS} increases by more than a factor of three but only small variations are obtained when varying the substitution rate (Table 4). However, smaller packing ratios are obtained for the more densely packed structures, as expected for lateral packing of chromophores. Furthermore, the depolarization ratios reflect the symmetry of the supramolecular organization of the substituents around the helix. Indeed, for the 1/3 substitution rate, the DR amounts to 4.89, a value close to 5, which characterizes systems with only one dominant diagonal β tensor component. The octupolar arrangements provide DR values close to the ideal value of 3/2. The Λ-shaped supramolecular structure is characterized by an intermediate value, which corresponds to a β_{XXZ}/β_{ZZZ} ratio of about 3, associated with an angle between the two CT axes (2θ) of $2\pi/3$ and a CT character smaller than 0.2.[49]

Subsequently, the size effects for substituted helices were addressed for the pyrimidine rings substituted by aniline groups. The appearance of the β_{HRS} curve is quite similar to the nonsubstituted case, but the β_{HRS} values are about one order of magnitude larger (Figure 8). Thus, helices with $n=$ 10–15 already present an optimal size with respect to maximizing the first hyperpolarizability. The β_{HRS} versus n curve

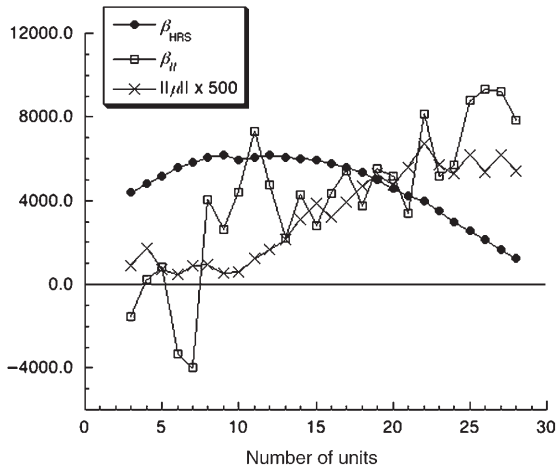

Figure 8. Evolution of β_{HRS}, $\beta_{\parallel}$ (au), and $||\mu||$ (D×500) as a function of the number of pyridine–pyrimidine units for the full (3/3) substitution pattern.

also supports the analysis attributing a larger periodicity to the substituted helices. In addition, the stability of the depolarization ratio with the helix size demonstrates the reinforcement of the NLO octupolar character (Figure 6). On the other hand, for $||\mu||$ and $\beta_{\parallel}$ the chain length dependencies are very different from the case of the nonsubstituted helices (Figure 8). Although not displayed here, the axial component of the first hyperpolarizability is not negligible and has an impact on the $\beta_{\parallel}$ value. This is partly due to the larger value of the axial component of the dipole moment, which increases almost monotonically with the helix size and further determines the components of the β tensor that are probed in $\beta_{\parallel}$. Furthermore, the reason for the lack of a regular pattern in the evolution of the first hyperpolarizability with the helix size is probably found in the disordered distribution of the chromophores, in particular those at the extremities that are subject to steric interactions only from one side.

Conclusion

The structure and the second-order nonlinear optical properties of a series of helical pyridine–pyrimidine oligomers

have been investigated theoretically. To this end 1) the OPLS-AA MM approach has been chosen for the optimization of geometries due to its good ability to reproduce the experimental structures and 2) the TDHF approach, based on the AM1 semiempirical Hamiltonian, has been employed to evaluate the first hyperpolarizabilities (β), the projection of the vector part of β on the dipole moment vector ($\beta_{\|}$) and the hyper-Rayleigh scattering response (β_{HRS}). In particular, we have investigated the impact of the size of the chain on β as well as the effects of the nature, position, and concentrations of donor/acceptor substituents.

In the absence of substituents the different quantities exhibit periodic variations with chain length, but the second-order NLO responses remain small. The first hyperpolarizabilities can, however, be enhanced by adding substituents, in particular when donor groups substitute the pyrimidine rings. When varying the concentrations of substituents, supramolecular assemblies with dipolar-, octupolar-, or Λ-shape NLO character can be built. Due to the packing effects, their second-order NLO responses are quite similar, whereas their depolarization ratios are clearly characteristic of their symmetry. This theoretical investigation therefore demonstrates the potential of helical structures to organize chromophores in such a way as to exhibit large second-order NLO responses in combination with specific depolarization ratios.

Possible extensions of this work include the use of larger lateral groups or chiral moieties, as well as substituents forming hydrogen-bonding networks. It would also be very informative to see whether our theoretical predictions are confirmed experimentally.

Acknowledgements

E.B. thanks the IUAP program number P5-03 for her postdoctoral grant. F.C. thanks Dr M. Kreissler for helpful discussions. B.C. thanks the Belgian National Fund for Scientific Research for his Research Director position. This work has benefited from a scientific cooperation established and supported by the Centre National de la Recherche Scientifique (CNRS), the FNRS, and the Commissariat Général aux Relations Internationales (CGRI) de la Communauté Wallonie-Bruxelles. The calculations were performed thanks to computing time made available by the SiMoA (Simulation et Modélisation en Aquitaine, France), the intensive calculation pole "M3PEC-MESOCENTRE" of the University of Bordeaux I, as well as by the Interuniversity Scientific Computing Facility (ISCF), installed at the Facultés Universitaires Notre-Dame de la Paix (Namur, Belgium), for which the authors gratefully acknowledge the financial support of the FNRS-FRFC and the "Loterie Nationale" for the Convention number 2.4578.02, and of the FUNDP.

[1] T. Nakano, Y. Okamoto, *Chem. Rev.* **2001**, *101*, 4013–4038.
[2] C. Bränden, J. Tooze, *Introduction to Protein Structure*, Garland, New York, **1991**.
[3] A. N. Aleshin, H. J. Lee, Y. W. Park, K. Akagi, *Phys. Rev. Lett.* **2004**, *93*, 196601.
[4] C. Schmuck, *Angew. Chem.* **2003**, *115*, 2552–2556; *Angew. Chem. Int. Ed.* **2003**, *42*, 2448–2452; .
[5] R. P. Sijbesma, E. W. Meijer, *Chem. Commun.* **2003**, 5–16.
[6] a) C. Dolain, V. Maurizot, I. Huc, *Angew. Chem.* **2003**, *115*, 2844–2846; *Angew. Chem. Int. Ed.* **2003**, *42*, 2738–2740; ; b) I. Huc, *Eur. J. Org. Chem.* **2004**, *2004*, 17–29; c) C. Dolain, J. M. Léger, N. Delsuc, H. Gornitzka, I. Huc, *Proc. Natl. Acad. Sci.* **2005**, *102*, 16146–16151.
[7] A. Tanatani, A. Yokoyama, I. Azumaya, Y. Takakura, C. Mitsui, M. Shiro, M. Uchiyama, A. Muranaka, N. Kobayashi, T. Yokozawa, *J. Am. Chem. Soc.* **2005**, *127*, 8553–8561.
[8] M. T. Stone, J. M. Heemstra, J. S. Moore, *Acc. Chem. Res.* **2006**, *39*, 11–20.
[9] J. M. Lehn, *Supramolecular Chemistry Concepts and Perspectives*, VCH, Weinheim, **1995**, Chapter 8.
[10] S. Hecht, *Mater. Today* **2005**, *8*, 48–55.
[11] J. Zhang, M. T. Albelda, Y. Liu, J. W. Canary, *Chirality* **2005**, *17*, 404–420.
[12] H. Zhao, F. Sanda, T. Masuda, *Polymer* **2006**, *47*, 1584–1589.
[13] T. J. Katz, L. Liu, N. D. Willmore, J. M. Fox, A. L. Rheingold, S. Shi, C. Nuckolls, B. H. Rickman, *J. Am. Chem. Soc.* **1997**, *119*, 10054–10063.
[14] T. Verbiest, S. Van Elshocht, M. Kauranen, L. Hellemans, J. Snauwaert, C. Nuckolls, T. J. Katz, A. Persoons, *Science* **1998**, *282*, 913–915.
[15] T. Verbiest, S. Sioncke, A. Persoons, L. Vyklick, T. J. Katz, *Angew. Chem.* **2002**, *114*, 4038–4040; *Angew. Chem. Int. Ed.* **2002**, *41*, 3882–3884.
[16] J. E. Field, T. J. Hill, D. Venkataraman, *J. Org. Chem.* **2003**, *68*, 6071–6078.
[17] a) S. Maiorana, A. Papagni, E. Licandro, R. Annunziata, P. Paravidino, D. Perdicchia, C. Giannini, M. Bencini, K. Clays, A. Persoons, *Tetrahedron* **2003**, *59*, 6481–6488; b) C. Baldoli, A. Bossi, C. Giannini, E. Licandro, S. Maiorana, D. Perdicchia, *Synlett* **2005**, 1137–1141.
[18] T. Iwasaki, Y. Kohinata, H. Nishide, *Org. Lett.* **2005**, *7*, 755–758.
[19] C. A. Daul, I. Ciofini, V. Weber, *Int. J. Quantum Chem.* **2003**, *91*, 297–302.
[20] E. Botek, B. Champagne, M. Turki, J. M. André, *J. Chem. Phys.* **2004**, *120*, 2042–2048.
[21] a) B. Champagne, J. M. André, E. Botek, E. Licandro, S. Maiorana, A. Bossi, K. Clays, A. Persoons, *ChemPhysChem* **2004**, *5*, 1438–1442; b) **2005**, *412*, 274–279; corrigendum: E. Botek, M. Spassova, B. Champagne, I. Asselberghs, A. Persoons, K. Clays, *Chem. Phys. Lett.* **2006**, *417*, 282.
[22] a) L. Brunsveld, E. W. Meijer, R. B. Prince, J. S. Moore, *J. Am. Chem. Soc.* **2001**, *123*, 7978–7984; b) J. van Gestel, P. van der Schoot, M. A. J. Michels, *Macromolecules* **2003**, *36*, 6668–6673; c) J. van Gestel, *Macromolecules* **2004**, *37*, 3894–3898; d) J. Tabei, M. Shiotsuki, F. Sanda, T. Masuda, *Macromolecules* **2005**, *38*, 5860–5867.
[23] J. van Gestel, A. R. A. Palmans, B. Titulaer, J. A. J. M. Vekemans, E. W. Meijer, *J. Am. Chem. Soc.* **2005**, *127*, 5490–5494.
[24] M. Ohkita, J. M. Lehn, G. Bauum, D. Fenske, *Chem. Eur. J.* **1999**, *5*, 3471–3481.
[25] L. A. Cuccia, J. M. Lehn, J. C. Homo, M. Schmutz, *Angew. Chem.* **2000**, *112*, 239–243; *Angew. Chem. Int. Ed.* **2000**, *39*, 233–237.
[26] M. Barboiu, J. M. Lehn, *Proc. Natl. Acad. Sci.* **2002**, *99*, 5201–5206.
[27] A. Petijean, L. A. Cuccia, J. M. Lehn, H. Nierengarten, C. Schmutz, *Angew. Chem.* **2002**, *114*, 1243–1246; *Angew. Chem. Int. Ed.* **2002**, *41*, 1195–1198; .
[28] M. Barboiu, G. Vaughan, N. Kyritsakas, J. M. Lehn, *Chem. Eur. J.* **2003**, *9*, 763–769.
[29] I. Odriozola, N. Kyritsakas, J. M. Lehn, *Chem. Commun.* **2004**, 62–63.
[30] a) J. Zyss, J. F. Nicoud, M. Coquillay, *J. Chem. Phys.* **1984**, *81*, 4160–4167; b) F. Pan, M. S. Wong, V. Gramlich, C. Bosshard, P. Günter, *J. Am. Chem. Soc.* **1996**, *118*, 6315–6316.
[31] a) This force field is a modified version of the parent MM2 from N. L. Allinger, *J. Am. Chem. Soc.* **1977**, *99*, 8127–8134; b) U. Bukert, N. L. Allinger, *Molecular Mechanics*, American Chemical Society: Washington, DC, **1982**.

[32] a) This force field is a modified version of the parent MM3 from N. L. Allinger, Y. H. Yuh, J. H. Lii, *J. Am. Chem. Soc.* **1989**, *111*, 8551–8566; b) J. H. Lii, N. L. Allinger, *J. Am. Chem. Soc.* **1989**, *111*, 8566–8575; c) J. H. Lii, N. L. Allinger, *J. Am. Chem. Soc.* **1989**, *111*, 8576–8582; N. L. Allinger, L. Yan, *J. Am. Chem. Soc.* **1993**, *115*, 11918–11925.

[33] a) This force field is a modified version of the parent AMBER from S. J. Weiner, P. A. Kollman, D. T. Nguyen, D. A. Case, *J. Comput. Chem.* **1986**, *7*, 230–252; b) D. Q. McDonald, W. C. Still, *Tetrahedron Lett.* **1992**, *33*, 7743–7746.

[34] a) W. L. Jørgensen, D. S. Maxwell, J. Tirado-Rives, *J. Am. Chem. Soc.* **1996**, *118*, 11225–11236; b) W. Damm, A. Frontera, J. Tirado-Rives, W. L. Jørgensen, *J. Comput. Chem.* **1997**, *18*, 1955–1970.

[35] J. J. P. Stewart, *J. Mol. Model.* **2004**, *10*, 6–12.

[36] M. J. S. Dewar, E. G. Zoebisch, E. F. Healy, J. J. P. Stewart, *J. Am. Chem. Soc.* **1985**, *107*, 3902–3909.

[37] a) J. J. P. Stewart, *J. Comput. Chem.* **1989**, *10*, 209–220; b) J. J. P. Stewart, *J. Comput. Chem.* **1989**, *10*, 221–264.

[38] J. J. P. Stewart, MOPAC, Fujitsu, **2002**.

[39] a) H. Sekino, R. J. Bartlett, *J. Chem. Phys.* **1986**, *85*, 976–989; b) S. P. Karna, M. Dupuis, *J. Comput. Chem.* **1991**, *12*, 487–504.

[40] a) D. R. Kanis, M. A. Ratner, T. J. Marks, *Chem. Rev.* **1994**, *94*, 195–242; b) J. L. Brédas, C. Adant, P. Tackx, A. Persoons, B. M. Pierce, *Chem. Rev.* **1994**, *94*, 243–278.

[41] a) F. Castet, B. Champagne, *J. Phys. Chem. A* **2001**, *105*, 1366–1370; b) E. Botek, B. Champagne, *Appl. Phys. B* **2002**, *74*, 627–634; c) M. Guillaume, E. Botek, B. Champagne, F. Castet, L. Ducasse, *Int. J. Quantum Chem.* **2002**, *90*, 1378–1387; d) M. Guillaume, B. Champagne, F. Castet, L. Ducasse, in *Computational Chemistry, Reviews of Current Trends, Vol. VIII* (Ed.: J. Leszczynski), World Scientific Publishing, Singapore, **2003**, Chapter 2, pp. 81–130; e) M. Guillaume, E. Botek, B. Champagne, F. Castet, L. Ducasse, *J. Chem. Phys.* **2004**, *121*, 7390–7400.

[42] a) B. Champagne, B. Kirtman, in *Nonlinear Optical Materials: Handbook of Advanced Electronic and Photonic Materials and Devices, Vol. 9* (Ed.: H. S. Nalwa), Academic Press, San Diego, **2001**, Chapter 2, pp. 63–126; b) B. Champagne, B. Kirtman, *J. Chem. Phys.* **2006**, *125*, 024101.

[43] R. Bersohn, Y. H. Pao, H. L. Frisch, *J. Chem. Phys.* **1966**, *45*, 3184–3198.

[44] F. Mohamadi, N. G. J. Richards, W. C. Guida, R. Liskamp, M. Lipton, C. Caufield, G. Chang, T. Hendrickson, W. C. Still, *J. Comput. Chem.* **1990**, *11*, 440–467.

[45] J. J. P. Stewart, MOPAC, Quantum Chemistry Program Exchange, 455.

[46] For the $n=8$ helix, a punctual calculation carried out using the B3LYP exchange-correlation functional and the 6–31G* basis set provides a value of 4.33 Å for the pitch and 13.37 Å for the length. Due to the important computational needs DFT geometry optimizations of other helices, as well as with other functionals, have not been performed.

[47] a) J. Zyss, I. Ledoux, *Chem. Rev.* **1994**, *94*, 77–105; b) T. Verbiest, K. Clays, C. Samyn, J. Wolff, D. Reinhoudt, A. Persoons, *J. Am. Chem. Soc.* **1994**, *116*, 9320–9323.

[48] C. R. Moylan, S. Ermer, S. M. Lovejoy, I.-H. McComb, D. S. Leung, R. Wortmann, P. Krdmer, R. J. Twieg, *J. Am. Chem. Soc.* **1996**, *118*, 12950–12955.

[49] M. Yang, B. Champagne, *J. Phys. Chem. A* **2003**, *107*, 3942–3951.

[50] B. Champagne, *Int. J. Quantum Chem.* **1997**, *65*, 689–696.

Received: April 18, 2006
Revised: August 3, 2006
Published online: October 18, 2006

